Romanian Reports in Physics, Vol. 59, No. 2, P. 457–472, 2007

Dedicated to Prof. Dorin N. Poenaru's 70th Anniversary

NUCLEON SPECTROSCOPY IN MESON PHOTOPRODUCTION

E. HOURANY

IN2P3,Institut De Physique Nucléaire, 91406 Orsay Cedex, France
E-mail: hourany@ipno.in2p3.fr

(Received February 23, 2007)

Abstracts. Nucleon spectroscopy studies the nucleon and its resonances. In photoproduction of mesons below a beam energy of 2 GeV, the main process is the excitation of nucleon resonances. This can be used to complement the study of these resonances, usually carried out with pion-nucleon scattering. A basic presentation of the lightest mesons and the resonances is done. The formalism of the pseudoscalar meson photoproduction is given. The data bases are described. Detailed developements in η and ω meson photoproduction on the proton are reported.

Key words: mesons, photoproduction, nucleon resonances.

1. **INTRODUCTION**

Much effort is being concentrated on the study of the resonances of the nucleon. The existing data for nucleon resonances were mostly determined by πN scattering. The comparison of the set of resonances predicted by modern quark models with the set of experimentally established resonances resulted in the so-called 'missing resonances' problem: more resonances are predicted than observed. This problem encouraged the use of the photoproduction of mesons as an alternative tool to excite the resonances. The advent of a new generation of electron accelerators allowed to perform meson photoproduction experiments of unprecedented sensitivity and precision. The new facilities are CLAS at TJNAF in Newport News, ELSA in Bonn, ESRF in Grenoble, MAMI in Mainz and SPring-8 in Osaka. At these places, photon beams were produced with high performances: (1) a high duty cycle allowing to perform coincidence experiments, (2) high intensity photon beams reaching $\approx 10^7$ γ/sec, (3) a high

energy crossing the threshold of η meson and kaon production, and (4) polarized targets and tagged and polarized beams allowing to perform precise experiments. In addition, 4π detectors were constructed with new electronics processing hundreds of parameters and new data-storing systems. The use of polarised beam or target can reveal the small contribution of resonances through the interference terms.

2. MESONS AND NUCLEON RESONANCES

Pions have been abundantly produced in proton accelerators, and in many places charged pions were collected and used as secondary beams. Pion scattering on a proton target has been chosen as the best tool to excite and to study the resonances of the nucleon. Nucleonic resonances are excited states of the nucleon with large mass width but with well defined spin, isospin and parity. Their identification and their characterization were carried out through the analysis of the pion-nucleon scattering data by partial-wave phase-shifts method. In this method, the excitation of a given resonance is searched with the amplitude behaviour of a specific partial wave in a characteristic plot called Argand diagram. Quark models of the nucleon, based on 3 constituent quarks were developed in a similar way than the shell model for nuclei. They could reproduce as excited states of the nucleon most of the known resonances with their spins, parities, and approximate masses. These models are refined through the interpretation of dynamical properties of the resonances, in particular, their coupling to the photons and the mesons.

In Table 1, there are the main characteristics of the lightest mesons, taken from the PDG tables [1]. The J^π of the pseudoscalar mesons (pions, eta, kaons) is 0^-. The J^π of the vector mesons (rho, omega) is 1^-. The isospin of pions, kaons and η is 1, 1/2 and 0 respectively. The isospin is 1 for ρ and 0 for ω. All of the mesons have a short lifetime ($\leq 10^{-7}$ s); however, $\pi^\pm$ and $K^\pm$ may have a path of several meters in the laboratory and then be detected with standard detectors similarly to stable charged particles, whereas η, η', ρ and ω decay almost at their production point. The last column gives the decay modes of highest branching ratios. It is worth mentionning that the rare decay modes, not given in the table, are used as special tools to test chiral perturbation theory and basic invariance principles.

In terms of quarks, mesons are constituted by quark-antiquark pairs. Eight mesons $\pi^\pm$, π°, η_o, $K^\pm$, K° and $\overline{K}^\circ$ form an octet and a singlet η_s in SU(3) of flavors u, d, and s. The physical η and η' are mixtures of η_o and η_s. The elements of the octet can be considered in some circumstances as Goldstone bosons associated to chiral symmetry breaking and therefore they

Table 1

Characteristics of the lightest mesons

Mesons	I	J^π	Mass (MeV)	Lifetime (sec)	Decay modes (%)
$\pi^\pm$	1	0^-	139.57	2.6×10^{-8} cτ= 7.8 m	$\mu\nu$ (99.99)
π°	1	0^-	134.98	8.4×10^{-17}	$\gamma\gamma$ (98.8); $e^+e^-\gamma$ (1.2)
η	0	0^-	547.45	5.5×10^{-19}	$\gamma\gamma$ (38.9); $3\pi^\circ$ (31.9); $\pi^+\pi^-\pi^\circ$ (23.6); $\pi^+\pi^-\gamma$ (4.88); $e^+e^-\gamma$ (0.5)
η'	0	0^-	957.77	3.3×10^{-21}	$\pi^+\pi^-\eta$ (43.7); $\rho^0\gamma$ (30.2); $\pi^\circ\pi^\circ\eta$ (20.8); $\omega\gamma$(3.0); $\gamma\gamma$ (2.1)
$K^\pm$	1/2	0^-	493.7	1.2×10−8 cτ= 3.7 m	$\mu\nu$ (63.5); $\pi\pi$ (21.2)
$\rho^\pm;\rho^0$	1	1^-	775.8	Γ = 150.3 MeV	$\pi\pi$ ($\approx$ 100)
ω	0	1^-	782.6	Γ = 8.5 MeV	$\pi^+\pi^-\pi^\circ$ (89.1);$\pi^\circ\gamma$(8.9); $\pi^+\pi^-$(1.7)

Table 2

Nucleonic resonances

$N^\star$	$l_{\pi N}$	I	J^p	$\Gamma(MeV)$	Branching ratio		
					πN %	$\pi\pi N$ %	ηN %
P11(1440)	1	1/2	$1/2^+$	250-450	60-70	30-40	
D13(1520)	2	1/2	$3/2^-$	110-135	50-60	40-50	
S11(1535)	0	1/2	$1/2^-$	100-200	35-55	01-10	30-55
D15(1675)	2	1/2	$5/2^-$	140-180	40-50	50-60	
...	...	...	...	...	...	...	...
Δ							
P33(1232)	1	3/2	$3/2^+$	115-125	> 99		
P33(1600)	1	3/2	$3/2^+$	250-450	10-25	75-90	
S31(1620)	0	3/2	$1/2^-$	120-180	20-30	70-80	
...	...	...	...	...	...	...	...

can be used in chiral QCD at low energy as known objects allowed to directly interact with quarks.

In Table 2, there are the main characteristics of the lightest resonances of the nucleon, split into two families, i.e., $N^\star$ of isospin 1/2 and Δ of isospin 3/2 [1]. The resonances are named by a letter and two indices (accompanied into parentheses by their masses in MeV) according to their original identification through their decay modes into a pion-nucleon system. The letter indicates the orbital angular momentum $l_{\pi N}$ of pion-nucleon system. The first index indicates twice the isospin I and the second index twice the total angular momentum J. In column 5, there is the mass width Γ, and in the last columns the branching ratios of their decay modes into πN, $\pi\pi N$ or ηN. In

fact, only $N^\star$ family resonances can decay into ηN under isospin conservation, since, because of the isospin null of η, the total isospin of ηN system has a unique value of 1/2. Two properties are of high interest in the table: the high branching ratio ($> 99\%$) of $P_{33}(1232)$ decay into πN and the large one (30–55%) of $S_{11}(1535)$ into ηN.

3. THEORETICAL FORMALISM FOR PSEUDOSCALAR MESONS

3.1. S-MATRIX

The S-matrix for the photoproduction of pseudoscalar mesons on the proton ($\gamma p \to M + N$) can be written in terms of the Lorentz-invariant matrix element $\mathcal{M}_{fi}$, the masses M, the four-component momenta p and the total energies E by[2, 3]:

$$S_{fi} = \frac{1}{(2\pi)^2}\left(\frac{M_p M_N}{4E_N E_M E_p E_\gamma}\right)^{1/2} \mathcal{M}_{fi} \times \delta^{(4)}(p_p + p_\gamma - p_M - p_N).$$

The matrix element can be expressed using Dirac spinors u and $\overline{u}$ by

$$\mathcal{M}_{fi} = \overline{u}\left[\sum_{j=1}^{4} A_j M_j\right] u,$$

where M_j are operators and A_j invariant amplitudes functions of Mandelstam variables s, t, and u.

The operators M_j are expressed in terms of the four-momenta, the polarization vector ϵ of the photon, and Dirac matrices γ_5 and γ by

$$M_1 = -\gamma_5 \gamma.\epsilon\gamma.p_\gamma, \quad M_2 = 2\gamma_5(\epsilon.p_p p_\gamma.p_N - \epsilon.p_N p_\gamma.p_p),$$

$$M_3 = \gamma_5(\gamma.\epsilon p_\gamma.p_p - \gamma.p_\gamma \epsilon.p_p), \quad M_4 = \gamma_5(\gamma.\epsilon p_\gamma.p_N - \gamma.p_\gamma \epsilon.p_N).$$

The matrix element can be as well expressed in Pauli space of two-component vectors v and $\overline{v}$

$$\mathcal{M}_{fi} = \left(\frac{E_N + M_N}{2M_N}\right)^{1/2} \left(\frac{E_p + M_p}{2M_p}\right)^{1/2} \overline{v} F v,$$

where the operator F is expressed in terms of Pauli matrices and momenta by

$$F = F_1 \sigma.\epsilon + F_2 i(\sigma.p_M)(\sigma.p_\gamma \times \epsilon) + F_3(\sigma.p_\gamma)(p_M.\epsilon) + F_4(\sigma.p_M)(p_M.\epsilon).$$

In Pauli space the amplitudes F_i are called CGLN amplitudes and are functions of the incident energy and the scattering angle. A given F_i can be expressed in terms of the 4 A_i and vice versa. Also, other families of amplitudes exist: helicity amplitudes, transversity amplitudes, etc.

The elementary cross section can be expressed in terms of the matrix element

$$d\sigma = (2\pi)^4 \frac{M_p M_N |\mathcal{M}_{fi}|^2 \delta^{(4)}(p_p + p_\gamma - p_M - p_N)}{4E_N E_M((p_p.p_\gamma)^2 - p_p^2.p_\gamma^2)^{1/2}} \times \frac{d^3p_M d^3p_N}{(2\pi)^6}.$$

3.2. OBSERVABLES

The cross section $d\sigma/d\Omega$ and other observables can be expressed in terms of the invariant amplitudes or the CGLN amplitudes or helicity amplitudes ... [2, 3]. The amplitudes in any set of amplitudes are complex numbers. So, 4 complex amplitudes allow to form 16 bilinear real numbers and therefore to calculate 16 observables. The 16 observables currently used are: (1) the differential cross section $d\sigma/d\Omega$, (2) the polarized beam asymmetry Σ, (3) the polarized target asymmetry T, (4) the recoil baryon polarization asymmetry P, (5–8) the four double polarization beam-target asymmetries E, F, G, and H, (9–12) the four double polarization beam-recoil asymmetries C_x, C_y, O_x, and O_y, and (13–16) the four double polarization target-recoil asymmetries T_x, T_z, L_x, and L_z.

It has been shown that among the 16 observables only seven were independent. Therefore, we need the measurement of the cross section $d\sigma/d\Omega$ and six asymmetry measurements to determine completely the scattering amplitude at each couple of incident energy E_γ and scattering angle θ.

3.3. EXPANSION INTO MULTIPOLES

The CGLN amplitudes can be expanded into a multipole decomposition:

$$F_1 = \sum_{L=0}^{\infty} (LM_L^+ + E_L^+)P'_{L+1}(x) + ((L+1)M_L^- + E_L^-)P'_{L-1}(x)$$

$$F_2 = \sum_{L=1}^{\infty} ((L+1)M_L^+ + LM_L^-)P'_L(x)$$

$$F_3 = \sum_{L=1}^{\infty} (E_L^+ - M_L^+)P''_{L+1}(x) + (E_L^- + M_L^-)P''_{L-1}(x)$$

$$F_4 = \sum_{L=2}^{\infty} (M_L^+ - E_L^+ - M_L^- - E_L^-)P''_L(x).$$

The interest of the multipole expansion is that near threshold the centrifugal barrier provides a natural truncation to multipoles of low L and that

baryon resonances are eigenstates of total angular momentum, parity and isospin and therefore can be associated to terms in the expansion.

The multipole notations are based on the total angular momentum and parity selection rules.

In the $\gamma p \to MN$ photoproduction reaction, the total angular momentum of the γ is J_γ and its parity is -1, whereas the spin and parity J^π of p, M, N are $\frac{1}{2}^+$, 0^-, and $\frac{1}{2}^+$, respectively. The orbital angular momentum in the γp system is L_γ and in the final MN system is L. The total angular momentum and parity conservation laws are writen:

$$J = J_\gamma \pm \frac{1}{2} = L \pm \frac{1}{2} \quad \text{and} \quad P = -(-1)^{L_\gamma} = -(-1)^L.$$

We have to take into account the two possible electric and magnetic interactions of the γ, yielding $J_\gamma = L_\gamma$ (magnetic) and $J_\gamma = L_\gamma \pm 1$ (electric).

It follows that:

– for a given L value, J could have either $L + \frac{1}{2}$ or $L - \frac{1}{2}$ value;

– for $J = L + \frac{1}{2}$, J_γ could have either the value L requiring a magnetic interaction to satisfy the parity conservation or the value $L + 1$ with electric interaction. The two corresponding terms in the multipole expansion will be denoted by M_L^+ and E_L^+ respectively;

– for $J = L - \frac{1}{2}$, J_γ will have either $L - 1$ or L giving similarly E_L^- and M_L^- respectively.

3.4. DYNAMICS

The formalism presented in this paper so far was derived from invariance principles and contains four free complex amplitudes functions of the incident energy and the scattering angle. The expansion in multipoles of these amplitudes allows to change the parametrization into another one, more adapted to real processes. The formalism is exact and model-independent. A complete description of the pseudoscalar meson photoproduction requires the determination of the amplitudes or their expansion into multipoles. One way for their determination is to achieve at each couple of energy and angle a complete measurement, i.e., the measurement of well chosen seven observables. The other way is to find out the dynamics of the process which yields an exact determination of these amplitudes, what is in fact the final goal of the physicist. At present, neither way was achieved, since on one hand, the measurements concern a very few observables in narrow energetic and angular ranges, and on the other hand, no exact dynamics exists for the process, but instead only dynamical models with more or less parameters tend to constrain the amplitudes.

In the isobar model [4], a few resonances with a background participate to meson photoproduction. The amplitudes of the partial waves are built on a coherent sum of the amplitudes of the resonances and of the background. There are required five parameters per resonance and four parameters for the background. This model was extensively used because of its simplicity and of the dominance of resonance excitation in the energy domain under 2 GeV. It suffers from the high number of parameters.

In the effective lagrangien approach of meson photoproduction [5, 6], at the tree level, a few Feynmann diagrams are taken into account: (1) s- and u-channel Born terms, (2) resonances in the s- and u-channels, and (3) vector meson exchange in the t-channel. One writes the interaction lagrangien for either of the two vertices of each diagram, attaching to them coupling constants to be determined by fitting experimental data. This approach is in principle more founded than the isobar model, since it allows to put on the same foot different diagrams and to use less parameters than the isobar model.

Recently, phenomenological chiral quark models appeared in pseudoscalar meson photoproduction [7]. In these models, pseudoscalar mesons are treated as Goldstone bosons, which are allowed to interact with quarks inside baryons. The number of parameters here is in principle one, even for all Goldstone bosons, since these are connected among themselves within SU(3) of flavor. These models use the wave functions of the quarks provided by constituent quark models [8, 9, 10, 11] and therefore constrain them through the comparison of the predictions to observables measured in meson photoproduction.

4. DATA BASE OF MESON PHOTOPRODUCTION

Recent experiments in meson photoproduction were performed exploring wider ranges of incident energy and scattering angles with higher kinematical and statistical precisions. Also several single or double polarization observables related to beam and target polarization were measured. The analysis and interpretation of the results have been mainly done within a regular updating of theoretical codes generated and controlled by several groups of theoreticians.

The GWU-Group with the SAID program [12] maintain updated data bases and multipole analyses of pion-nucleon scattering and pion photoproduction. The MAID code, based on a unitary isobar model with a partial wave analysis of pion photo- and electroproduction [13], fits the world data and give predictions for multipoles, amplitudes, cross sections and polarization observables in the energy range from pion threshold up to $W = 2$ GeV and photon virtuality $Q^2 \leq 5$ GeV^2. Besides the MAID program for pions

there is a series of program for photo- and electroproduction of the other pseudoscalar mesons. G. Penner and U. Mosel analysed in a coupled-channel all pion- and photon-induced experimental data for energies up to $\sqrt{s} = 2$ GeV. A.V. Anisvich et al. analysed the photoproduction data on $\gamma p \rightarrow \pi N, \eta N, K\Lambda$ and $K\Sigma$, with an isobar model. The rich information on the resonances extracted from the recent experiment data and their analysis can be found for instance in reference [16].

Beyond improving and completing the tables of nucleon resonances, the data and the models are used to test basic invariances such the sum rules or to solve some new physics cases.

For instance, the GDH sum rule relating the anomalous magnetic moment κ, the elementary charge e and nucleon mass M to the difference in the total photoabsorption cross sections for circularly polarized photons on longitudinally polarized nucleons is

$$I_{GDH} = \int_{\nu_0}^{\infty} \frac{\sigma_{1/2} - \sigma_{3/2}}{\nu} d\nu = -\frac{\pi e^2}{2M^2}\kappa^2,$$

where $\sigma_{1/2}$ and $\sigma_{3/2}$ are the photoabsorption cross sections for the helicity states $1/2$ and $3/2$ respectively, with ν being the photon energy. For the proton (neutron) target the equation predicts -205 (-233) μb. The integral was measured at Mainz from 200 to 800 MeV on proton target and has been found $-226\pm5\pm12$. The SAID and MAID codes give in single-pion photoproduction for the same energy interval -193 and -175 respectively. Clearly contributions beyond single-pion photoproduction should be taken into account [12].

An example of physics case was the pentaquark. In the past, some experimental and theoretical searches focused on pentaquarks, which are baryons with a minimal $qqqq\overline{q}$ structure. In 1997, Diakonov *et al.* [17] made definite predictions about the masses and widths of an antidecuplet of pentaquark states in the framework of a chiral soliton model. The mass widths predicted by the model are very narrow (10–15 MeV). If such states exist they should be directly visible in experimental invariant mass spectra. In 2003, the LEPS collaboration announced the experimental evidence of a first pentaquark θ^+ decaying into K^+n [18]. This was followed by positive or negative evidence from other experiments having previously collected data for other purposes. A second generation of dedicated photoproduction experiments, optimized for the pentaquark search was performed at Jefferson Lab. No evidence of a narrow peak has been seen in the invariant mass spectrum of K^+n produced on a proton or deuterium target with a photon beam ranging from 0.8 to 3.8 GeV [19, 20, 21].

5. BASIC EXPERIMENTS IN η MESON PHOTOPRODUCTION

The η-meson has isospin $I = 0$ and in consequence the isospin conservation makes that only the N^* of $I = 1/2$ can be excited through $\gamma p \to p\eta$ reaction. Precise experiments at MAMI, the microtron of Mainz, measured the total and the differential cross sections of η photoproduction on the proton, from threshold (707 MeV) until 790 MeV [22]. The differential cross sections were deduced from the analysis of the $\eta \to 2\gamma$ decay mode. The angular distributions were fitted by the usual expression:

$$d\sigma(\theta)/d\Omega = \frac{q}{k}[A + B\cos(\theta) + C\cos^2(\theta)].$$

Near threshold, the energy dependence of the total cross section is given by $(E_\gamma - E_{th})^{l+1/2}$, where l is the order of the dominant multipole. The experimental total cross section behaviour showed a $(E_\gamma - E_{th})^{1/2}$ dependence and the angular distributions of the differential cross sections were quasi isotropic. Both results infer that the s-wave E_{0^+} multipole is dominant.

The dominance of the S_{11} resonance allows to expand the cross section in terms proportional to the E_{0^+} multipole:

$$\frac{d\sigma}{d\Omega} = \frac{q^\star_\eta}{k^\star}\Big\{E^2_{0^+} - \ Re[E^\star_{0^+}(E_{2^-} - 3M_{2^-}) -$$
$$-2Re[E^*_{0^+}(3E_{1^+} + M_{1^+} - M_{1^-})]\cos(\theta) + 3Re[E^\star_{0^+}(E_{2^-} - 3M_{2^-})]\cos^2(\theta)\Big\}.$$

As the value of the coefficient B given by the fit is very small ($\leq 1\%$ of A) no significant contribution is found from P_{11} resonance involved only in the term of $\cos(\theta)$. On the other hand, the coefficient C of $\cos^2(\theta)$ is originating from the D_{13} resonance. Its significant value of $\approx$10% of A indicates that D_{13} clearly contributes. So, the major results of the MAMI experiment were: (1) to give precise cross section values near threshold, and (2) to rule out the possible contribution of the $P_{11}(1440)$ to the photoproduction of η.

At GRAAL experiment [23] the beam asymmetry Σ was measured for the reaction $\vec{\gamma}p \to \eta p$ using the linearly polarized photon beam. The expression of Σ is given by: $\sigma/\sigma_0 = 1 - P\Sigma\cos(2\phi)$, where σ and σ_0 are the differential cross sections with polarized and unpolarized beams respectively, P is the polarization of the beam and ϕ is the angle between the polarization and reaction plane. The polarization was switched alternatively between vertical and horizontal states. The two corresponding azimutal distributions of the reaction plane, N_{ver} and N_{hor}, normalized by the primary photon fluxes would give the following characteristic dependency on ϕ:

$$\sigma/\sigma_0 = \frac{2N_{ver}}{N_{ver} + N_{hor}} = 1 - P\Sigma\cos(2\phi).$$

The fit of the experimental distribution $\frac{2N_{ver}}{N_{ver}+N_{hor}}$ by an expression $1 - K\cos(2\phi)$ yields the coefficient K. Taking $K = P\Sigma$ and knowing P, one deduces Σ. The beam asymmetry Σ was plotted against θ_{cm} of the η for six bins of energy ranging from the threshold up to 1 100 MeV [23], Large positive asymmetries were obtained. The results were, on one hand, compared to predictions given by two independent calculations and, on the other hand, fitted in the frame of an isobaric model [23]. The comparison of these very precise and constraining results with various models confirmed the dominance of $S_{11}(1535)$ with contributions from $D_{13}(1520)$, $P_{13}(1720)$ and $D_{15}(1675)$.

At the tagged photon facility PHOENICS of the Bonn accelerator ELSA, a measurement of the target asymmetry of the reaction $\gamma p \to p\eta$ from threshold to 1150 MeV has been performed, using a frozen spin target with butanol (C_4H_9OH) as target material [24]. The determination of the target asymmetry T off the proton is given in the expression of the differential cross section for polarized nucleons σ_p:

$$\sigma_p = \sigma_0\{1 + p_y T \sin\phi\},$$

where σ_0 is the unpolarized differential cross section off the proton, p_y designates the polarization value of the target and ϕ is the angle between the target spin and the plane of the primary photon and the produced meson. The authors derived the relation for T in terms of the count rates belonging to different polarization states $(N_\uparrow, N_\downarrow)$:

$$T = \frac{1}{k}\frac{N_\uparrow - N_\downarrow}{p_\downarrow N_\uparrow \sin\phi + p_\uparrow N_\downarrow \sin\phi}.$$

Near threshold the angular distribution has a a change in sign at $\Theta_{CM} = 90^\circ$. This behaviour appears in the expression of T into leading multipoles:

$$T = -\frac{1}{\sigma_0} 3 \sin\theta\cos\theta\, Im[E_{0+}(E_{2-} + M_{2-}).$$

The interference of the dominant E_{0+} multipole (corresponding to the $S_{11}(1535)$ with the D-wave multipoles (E_{2-} and M_{2-}) which contain the contribution of the $D_{13}(1520)$ MeV leads to an angular structure proportional to $\sin\theta\cos\theta$. This behaviour is apparently contained in the data.

A simultaneous interpretation was performed for the three sets of observables, $d\sigma/d\Omega$ measured at Mainz, the target asymmetry T measured at Bonn and the beam asymmetry Σ of GRAAL. Two groups, using effective Lagrangien models performed an almost model-independent calculation based on an expansion into multipoles near the threshold of the transition amplitudes [25, 26]. Under the assumption of the dominance of s-wave and the additional contribution of p- and d- waves only by their interference with s-wave, the expansion could be limited to a few terms. Simple expressions of the

three observables $d\sigma/d\Omega$, T and Σ are obtained. The fit of the 3 sets of data by these expressions determine the coefficients into the expansion and hence the multipoles. In Fig. 1, the dashed and dotted lines are predictions of an effective Lagrangien model corresponding to calculations with and without D_{13} respectively. While the two calculations give similar results for $d\sigma/d\Omega$ and T, they give a dramatic change for Σ: without D_{13}, values close to zero and even negative are found, and, with D_{13}, values compatible with the experimental ones are seen. In addition, not only the agreement is poor in T, but also the theoretical result does not show a nodal angular structure at low energy.

The continuous line is the result of the fit by the expansion into multipoles. This fit reproduces the 3 sets of observables, nevertheless with two drawbacks: the high values of Σ at high energies and forward angles are not reproduced even after allowing the contribution of higher waves through an additional term in the expression of Σ, and the fit of the nodal structure is possible only at the expenses of the wrong sign in the phase between S_{11} and D_{13}. The authors claimed the confirmation of the experimental results in T and when extracting numerical values for various basic quantities they carried out results in two cases, case 1 for the 3 observables fitted together and case 2 for $d\sigma/d\Omega$ and Σ.

The extracted values of the branching ratio of D_{13} into η are 0.08 ± 0.01 and 0.05 ± 0.02 in cases 1 and 2 respectively, close to the prediction of the quark model, which is of 0.09. As to the helicity amplitude $A_{1/2}$ and the ratio $A_{3/2}/A_{1/2}$ for the excitation of D_{13}, they were found equal, in the two cases, to the following values:

$A_{1/2} = -79 \pm 9$ (to be compared to -24 ± 9 of the PDG tables),
$A_{3/2}/A_{1/2} = -2.1 \pm 0.2$ (to be compared to -6.9 ± 2.6 of the PDG tables).

This striking disagreement between these quantities extracted in η photoproduction of D_{13} and those of PDG tables based on pion photoproduction results has been previously found in the extraction of $A_{1/2}$ for S_{11} from η photoproduction using an expansion into multipoles near the threshold.

More recently, the study of η photoproduction was extendied to higher photon beam energies [27, 28, 29]. Differential and total cross sections were obtained up to 3 GeV beam energy. In references [27, 28] a quark model including the known resonances and a vector-meson exchange in the t-channel [30] and an isobar model including Born terms, vector meson exchange and resonances (ETA-MAID) [31] were used for the interpretation. In reference [29] partial wave amplitudes constructed in the framework of the operator expansion method [32] are used to fit the data. The finding was that the important contributions to the total cross section come from the resonances $S_{11}(1535)$, $P_{13}(1720)$ and $D_{15}(2070)$ while smaller contributions come from $S_{11}(1650)$ and $P_{13}(2200)$. It is expected that further experiments with polarized beams and

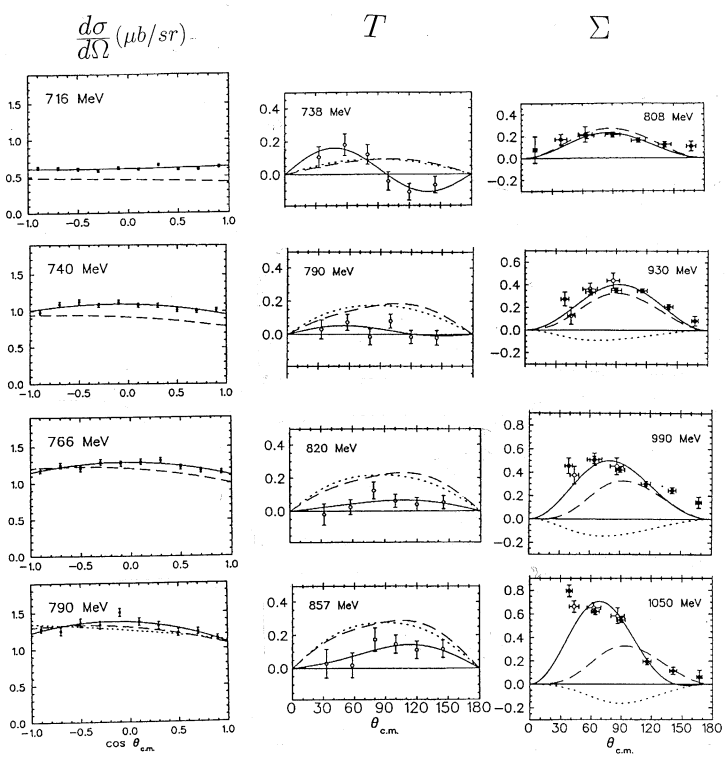

Fig. 1 – Cross section $d\sigma/d\Omega$ of Mainz, target asymmetry T of Bonn and beam asymmetry Σ of GRAAL of the reaction $\gamma p \to \eta p$ and their interpretation given in reference [26].

targets could confirm this finding and give evidence to additional resonances decaying into $N\eta$ and having small contributions to the total cross section.

6. BASIC EXPERIMENTS IN ω MESON PHOTOPRODUCTION

There is no nucleon resonance well-established decaying into vector mesons ω. The identification of ω with its narrow width (8 MeV) is easy. Also since the isospin of ω is zero, only the isospin $-1/2$ nucleon resonances can couple to the ωN channel. A search of resonant contribution in the ω photoproduction has recently seen a strong revival. In ω meson photoproduction at GRAAL experiment [33], the identification and selection of the events were carried out for the case of the ω-decay into three pions (branching ratio of 89%):

$$\gamma \ \mathrm{p} \to \mathrm{p} \ \omega \qquad \omega \to \pi^+\pi^-\pi^0.$$

With a linear polarization of the photons, the distribution of the angles θ and ϕ of the normal to the decay plane of ω in the rest frame of ω is [34]:

$$W = W^0(\cos\theta, \phi) - P_\gamma \cos(2\Phi) W^1(\cos\theta, \phi) - P_\gamma \sin(2\Phi) W^2(\cos\theta, \phi),$$

where, Φ is the angle between the production plane of ω and the polarization of the beam, P_γ is the degree of polarization of the beam, and the expressions W^0, W^1,W^2 are functions of spin density matrix elements ρ^α_{ik} which are to be determined by fitting the experimental data and to be compared to values extracted from theoretical models. These matrix elements are in fact double polarization beam-ω meson observables.

Integrating $W(\cos\theta, \phi, \Phi)$ over θ and ϕ yields:

$$W(\Phi) = 1 + P_\gamma . \frac{2\rho^1_{11} + \rho^1_{00}}{2\rho^0_{11} + \rho^0_{00}} . \cos(2\Phi).$$

The beam asymmetry Σ is extracted by fitting at each couple of incident energy and θ_ω angle bins the Φ distribution by an expression $K(1+$ $+P_\gamma \Sigma \cos(2\Phi))$. These Σ values are compared to the analog theoretical ones $\frac{2\rho^1_{11}+\rho^1_{00}}{2\rho^0_{11}+\rho^0_{00}}$ obtained in a quark model [35]. In this model an effective Lagrangian is used to study the s- and u-channel resonance contributions.

$$L_{eff} = -\overline{\psi}\gamma_\mu p^\mu \psi + \overline{\psi}\gamma_\mu e_q A^\mu \psi + \overline{\psi}\left(a\gamma_\mu + \frac{ib\sigma_{\mu\nu}q^\nu}{2m_q}\right)\phi^\mu_m \psi,$$

where ψ and $\overline{\psi}$ represent the quark and antiquark fields and ϕ^μ_m denotes the vector meson field. The two parameters a and b represent the vector and tensor couplings of the quark to the vector meson and $m_q = 330$ MeV is the constituent quark mass. The t-channel natural parity exchange is taken into account through the Pomeron exchange, while the unnatural parity exchange is described by the π° exchange. The results of this model are consistent with the known characteristics of ω meson photoproduction at high energies, i.e., a dominance of Pomeron and π° exchanges in the total cross section with a forward diffractive peaking in the differential cross sections.

In Fig. 2, the total cross section is shown. The GRAAL data (solid dots), are obtained by the integration of the differential cross sections. The error bars come mainly from the uncertainty at the limits of the integration. The systematic error of 5% is not shown. Similar to the previous existing data (shown with empty symbols), a strong rise at threshold is seen in GRAAL data. Moreover, a bump structure appears near threshold before the total cross section levels off to a value of $\approx$7.5 μb at 1.45 GeV. The model of Zhao *et al.* (solid line) satisfactorily reproduces the GRAAL data, and in particular among its different transition processes (shown in the figure) the resonant term is dominant near threshold and remains sizeable up to $E_\gamma = 2$ GeV. The same

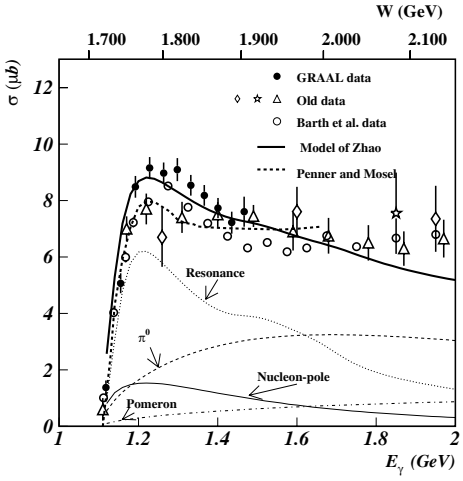

Fig. 2 – Total cross section of $\gamma p \to p\omega$ [33]. The calculations by Zhao are shown with several lines: solid for the full calculation, and other line types for contributing terms. The thicker dashed line is the calculation of Penner and Mosel [14].

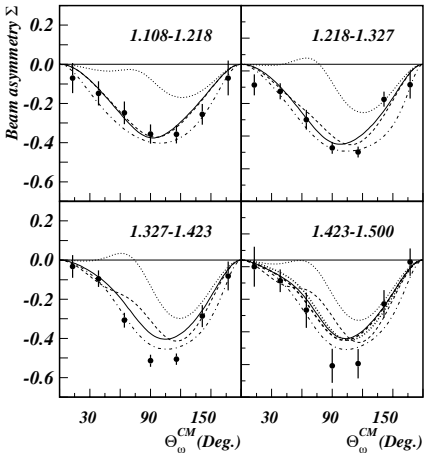

Fig. 3 – Beam asymmetry of $\gamma p \to p\omega$ for GRAAL data [33]. Zhao model: solid line for full calculation; dashed for no $D_{13}(1520)$ contribution; dotted for no $P_{13}(1720)$; dot-dashed for no $F_{15}(1680)$; heavy-dashed for no $F_{15}(2000)$; heavy-dotted for no $P_{13}(1900)$.

structure is also seen in the results of Barth *et al.* [36] plotted in empty circles and in the calculation of Penner and Mosel [14] (shown by the heavy dashed line), where the enhancement near threshold is attributed by the authors to $P_{11}(1710)$ and $P_{13}(1900)$ contributions.

In Fig. 3, the beam asymmetry of GRAAL data are presented showing large negative values while Σ should be vanishing without s- and u-channel transitions, particularly the excitation of resonances. The interpretation by Zhao et al. gives with solid lines, the full calculation results and, with other line types, the results when one single resonance is switched off (keeping the relative strengths of the remaining resonances as imposed by the quark model). So, some of the resonances, e.g. $D_{13}(1520)$, $P_{13}(1720)$, $F_{15}(1680)$, are found to play an indispensable role, and some effects due to the $F_{15}(2000)$ are also seen. In particular, the model suggests that $P_{13}(1720)$ plays an important role near threshold despite a small branching ratio 0.002 while the $P_{13}(1900)$ and $F_{15}(2000)$ have sizeable branching ratios, 0.1 and 0.4, but small contributions to the cross section. Also, recent results from SAPHIR gave the angular distributions of the decay products of ω meson in its rest frame and deduced a set of spin density matrix elements [36]. These results suggest also the excitation of some resonances in ω photoproduction channel.

7. SUMMARY

The photoproduction of the lightest mesons is a tool complementing the pion-nucleon scattering to study the baryon resonances. The formalism is well established and the relevant observables are well defined. Experiments and dynamical models have gained a revival motivated by the high accuracy which became reachable in the experiments and by the need of quark models to new constraints. Extension of the experiments are being undertaken (i) to involve the measurements of the single and double polarization of the beam and the proton target, (ii) to use neutron target (neutron weakly bound in the deuterium) or medium and heavy nuclei targets.

In nucleon spectroscopy, all the characteristics of the nucleon and its resonances are studied in the response of the nucleon as a whole (compound system) to external interactions. Another way to explore the nucleon is to study directly its internal structure through a new probe able to see the partons inside it. Presently, experiments are planned at several GeV of electron beams to study the generalized parton distribution (GPDs) describing the structure of the nucleon at the quark-gluon level.

REFERENCES

1. S. Eidelman *et al.*, Phys. Lett., **B 592**, 1 (2004).
2. R.A. Adelseck, B. Saghai, Phys. Rev., **C 42**, 108 (1990).
3. C.G. Fasano, F. Tabakin and B. Saghai, Phys. Rev., **C 46**, 2430 (1992).
4. H.R. Hicks *et al.*, Phys. Rev., **D 7**, 26141973.
5. M. Benmerrouche *et al.*, Phys. Rev., **D 51**, 32371995.
6. G. Knochlein *et al.*, Z. Phys. , **A 352**, 327 (1995)
7. Zhenping Li, Phys. Rev., **D 50**, 56391994; Phys. Rev., **D 52**, 4961995.
8. R. Koniuk and N. Isgur, Phys. Rev., **D 21**, 18681980.
9. C.P. Forsyth and R.E. Cutkosky, Z. Phys., **C 18**, 2141983.
10. D.M. Manley and E.M. Saleski, Phys. Rev., **D 45**, 40021992.
11. S. Capstick, Phys. Rev., **D 46**, 28641992.
12. R.A. Arndt *et al.*, Phys. Rev., **C 53**, 430 (1996) and **C66**, 055213 (2002).
13. $***$, MAID programs at `http://www.kph.uni-mainz.de/MAID`
14. G. Penner and U. Mosel, Phys. Rev., **C 66**, 055211–1 and 055212–1 (2002).
15. A.V. Anisovich *et al.*, Eur. Phys. J., **A 25** 427–439 (2005).
16. R. A. Arndt *et al.*, Phys. Rev., **C 74**, 045205 (2006).
17. D. Diakonov, V. Petrov and M. Polyakov, Z. Phys., **A 359**, 305 (1997).
18. T. Nakano *et al.*, Phys. Rev. Lett., **91**, 012002 (2003).
19. S. Niccolai *et al.*, Phys. Rev. Lett., **97**, 032001 (2006).
20. B. McKinnon *et al.*, Phys. Rev. Lett., **96**, 212001 (2006).
21. M. Battaglieri *et al.*, Phys. Rev. Lett., **96**, 042001 (2006).
22. B. Krusche *et al.*, Phys. Rev. Lett., **74**, 37361995
23. J. Ajaka *et al.*, Phys. Rev. Lett., **81**, 17971998.

24. A. Bock *et al.*, Phys. Rev. Lett., **81**, 5341998
25. N. C. Mukhopadhyay and N. Mathur, Phys. Lett., **B 444**, 7 (1998).
26. L. Tiator *et al.*, Phys. Rev., **C 60**, 035210–1.
27. F. Renard *et al.*, Phys. Lett., **B 528**, 215–220 (2002).
28. M. Dugger *et al.*, Phys. Rev. Lett., **89**, 222002–1.
29. V.Credé *et al.*, Phys. Rev. Lett., **94**, 012004–1.
30. B. Saghai and Z. Li , Eur. Phys. J., **B 11**, 217 (2001).
31. W.T.Chiang *et al.*, Phys. Rev., **C 68**, 045202 (2003).
32. A.V. Anisovich *et al.*, Eur. Phys. J., **A 24**, 111–128 (2005).
33. J. Ajaka *et al.*, Phys. Rev. Lett., **96**, 132003 (2006).
34. K. Schilling, P. Seyboth and G. Wolf, Nucl. Phys., **B 15**, 397–412 (1970).
35. Q. Zhao, Phys. Rev., **C 63**, 025203 (2001).
36. J. Barth *et al.*, Eur. Phys. J., **A 18**, 117–127 (2003).